Journal of Organometallic Chemistry 696 (2011) 1057–1065

Contents lists available at ScienceDirect

Journal of Organometallic Chemistry

journal homepage: www.elsevier.com/locate/jorganchem

Targeting nitric oxide synthase with ^{99m}Tc/Re-tricarbonyl complexes containing pendant guanidino or isothiourea moieties☆

Bruno L. Oliveira [a], Paula D. Raposinho [a], Filipa Mendes [a], Isabel C. Santos [a], Isabel Santos [a], António Ferreira [b], Carlos Cordeiro [b], Ana P. Freire [b], João D.G. Correia [a,*]

[a] Unidade de Ciências Químicas e Radiofarmacêuticas, ITN, Estrada Nacional 10, 2686-953 Sacavém, Portugal
[b] Centro de Química e Bioquímica, Departamento de Química e Bioquímica, Faculdade de Ciências da Universidade de Lisboa, Portugal

ARTICLE INFO

Article history:
Received 11 August 2010
Received in revised form
1 September 2010
Accepted 4 September 2010

Keywords:
Bioorganometallics
Guanidines
Isothioureas
Nitric oxide synthase
Rhenium
Technetium

ABSTRACT

The visualization of inducible nitric oxide synthase (iNOS) *in vivo* with specific radioactive probes could provide a valuable insight into the diseases associated with upregulation of this enzyme. Aiming at that goal, we have synthesized a novel family of conjugates bearing a pyrazolyl-diamine chelating unit for stabilization of the *fac*-$[M(CO)_3]^+$ core (M = ^{99m}Tc, Re) and pendant guanidino (**L^1** = guanidine, **L^2** = *N*-hydroxyguanidine, **L^3** = *N*-methylguanidine, **L^4** = *N*-nitroguanidine) or S-methylisothiourea (**L^5**) moieties for iNOS recognition. **L^1**–**L^5** reacted with *fac*-$[M(CO)_3(H_2O)]^+$, yielding complexes of the type *fac*-$[M(CO)_3(k^3\text{-L})]^+$ (M = Re/^{99m}Tc; **1**/**1a**, L = **L^1**; **2**/**2a**, L = **L^2**; **3**/**3a**, L = **L^3**; **4**/**4a**, L = **L^4**; **5**/**5a**, L = **L^5**), which were fully characterized by the usual analytical methods in chemistry and radiochemistry, including X-ray diffraction analysis in the case of **1**. The rhenium complexes **1**–**5** were prepared as "cold" surrogates of the ^{99m}Tc(I) complexes. Enzymatic assays with murine purified iNOS demonstrated that **L^1**, **L^2**, **1** and **2** are poor NO-producing substrates. These assays have also shown that metallation of **L^4** and **L^5** ($K_i > 1000$ μM) gave complexes with increased inhibitory potency (**4**, $K_i = 257$ μM; **5**, $K_i = 183$ μM). The organometallic rhenium complexes permeate through LPS-treated RAW 264.7 macrophage cell membranes, interacting specifically with the target enzyme, as confirmed by the partial suppression of NO biosynthesis (*ca.* 20% in the case of **4** and **5**) in this cell model. The analog ^{99m}Tc(I)-complexes **1a**–**5a** are stable *in vitro*, being also able to cross cell membranes, as demonstrated by internalization studies in the same cell model with compound **4a** (4h, 37 °C; 33.8% internalization). Despite not being as effective as the α-amino-acid-containing metal-complexes previously described by our group, the results reported herein have shown that similar ^{99m}Tc(I)/Re(I) organometallic complexes with pendant amidinic moieties may hold potential for targeting iNOS expression *in vivo*.

1. Introduction

Nitric oxide (NO) is a key signaling mammalian mediator produced *in vivo* by oxidation of L-arginine to L-citrulline catalyzed by Nitric Oxide Synthase (NOS), which has two constitutive isoforms (neuronal, nNOS; endothelial, eNOS) and one inducible isoform (iNOS) [1–4]. Localized overproduction of NO resulting from NOS upregulation has been also associated to several diseases, including cancer (e.g. breast and prostate), neurological disorders or vascular malfunctions, among others [5–7]. Therefore, noninvasive imaging of NOS expression *in vivo* holds potential for understanding NO/NOS-related diseases, and may facilitate the development of novel therapeutic approaches [8,9]. Considering that the nuclear imaging techniques Single Photon Emission Tomography (SPECT) and Positron Emission Tomography (PET) display a set of superior features for clinical application (e.g. high sensitivity and unlimited depth penetration), research on specific radioactive probes based on β^+-emitters for the *in vivo* targeting of NOS has been reported [10,11]. Owing to its almost ideal nuclear properties ($t_{1/2}$ = 6.02 h, $E_{\gamma max}$ = 140 keV), ready availability from a ^{99}Mo/^{99m}Tc generator, and varied (radio)chemistry, technetium-99m (^{99m}Tc) is currently the most used radionuclide in diagnostic procedures (SPECT imaging) in nuclear medicine [12,13]. In the past few years we have been involved in the design and biological evaluation of novel ^{99m}Tc(I)-complexes for probing molecular targets *in vivo* [14–16], namely the inducible form of NOS [17,18]. Those studies led to the

☆ Special Issue: 5th International Symposium on Bioorganometallic Chemistry – ISBOMC10. July 5th–9th 2010 Bochum, Germany.

* Corresponding author. Tel.: +351219946233.
E-mail address: jgalamba@itn.pt (J.D.G. Correia).

0022-328X/$ – see front matter © 2010 Elsevier B.V. All rights reserved.
doi:10.1016/j.jorganchem.2010.09.019

introduction of a set of bioorganometallic complexes of the type *fac*-[M(CO)$_3$(k^3-L)] (M = ^{99m}Tc, Re) stabilized by a pyrazolyl-diamine chelating unit, and containing a pendant NOS substrate (L-arginine) or NOS inhibitor (L-arginine analogs: N^{ω}-CH$_3$- or N^{ω}-NO$_2$-L-arginine) (Fig. 1) [17,18].

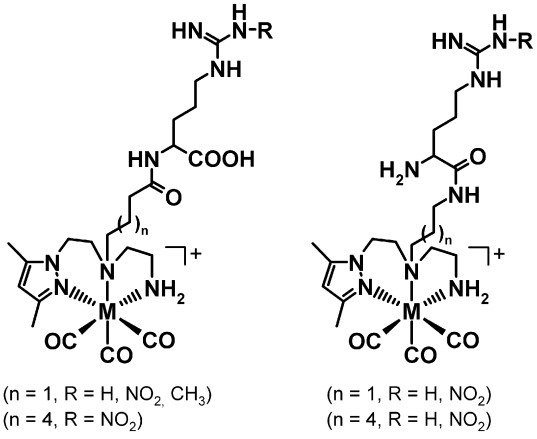

Fig. 1. Bioorganometallic complexes of the type *fac*-[M(CO)$_3$(k^3-L)] (M = ^{99m}Tc, Re) containing a pendant NOS substrate (L-arginine) or NOS inhibitor (N^{ω}-CH$_3$- or N^{ω}-NO$_2$-L-arginine).

The rhenium complexes with the pendant N^{ω}-NO$_2$-L-arginine unit inhibited iNOS, being their inhibitory capacity similar to that of free N^{ω}-NO$_2$-L-arginine in some cases. These complexes permeate also through activated RAW 264.7 macrophage cell membranes, suppressing NO biosynthesis. The analog ^{99m}Tc(I)-complexes presented also the ability to cross cell membranes, as demonstrated by internalization studies in the same cell model [18]. Brought together, these studies have demonstrated the importance of the structural parameters in the interaction of the organometallic complexes with the enzyme active site. The knowledge of the molecular determinants underlying such interaction will, ultimately, allow the design of ^{99m}Tc(I)/Re(I)-complexes with better iNOS targeting properties. Aiming to draw a preliminary relationship between the structure of the Re/^{99m}Tc organometallic complexes and their affinity for the NOS active site, we decided to study the enzyme recognition properties of metal-complexes where the α-amino-acid function is absent. It is known that close analogs of L-arginine and non α-amino-acid *N*-alkyl-*N*′-hydroxyguanidines are NOS substrates for NO biosynthesis [19,20]. Additionally, various non-aminoacid-based inhibitors of NOS, which may be divided into two principal families (amidinic and heterocyclic compounds), have been synthesized aiming to improve the selectivity and therapeutic profile of L-arginine derivatives. Among the numerous elements of the amidinic family, the guanidine and the isothiourea derivatives have been the most explored from a biological point of view [21]. Herein, we describe the synthesis and characterization of novel ^{99m}Tc(I)/Re(I)-complexes containing various pendant guanidino or S-methylisothiourea moieties for NOS recognition. We will also report on the enzymatic activity of iNOS in the presence of the compounds, and assess their ability to influence NO biosynthesis in LPS-activated macrophages.

2. Results and discussion

2.1. Synthesis and characterization of L^1–L^5

The new conjugates $\mathbf{L^1}$–$\mathbf{L^5}$ contain a pyrazolyl-diamine chelating unit for stabilization of the *fac*-[M(CO)$_3$]$^+$ core (M = ^{99m}Tc, Re) and pendant guanidino ($\mathbf{L^1}$ = guanidine, $\mathbf{L^2}$ = *N*-hydroxyguanidine, $\mathbf{L^3}$ = *N*-methylguanidine, $\mathbf{L^4}$ = *N*-nitroguanidine) or S-methylisothiourea ($\mathbf{L^5}$) groups, which are expected to recognize the active site of iNOS. *tert*-butyl 2-((3-aminopropyl)(2-(3,5-dimethyl-1*H*-pyrazol-1-yl)ethyl)amino)ethylcarbamate (**pzC$_3$NH$_2$NH-Boc**) was used as the common precursor for the preparation of all conjugates (Scheme 1) [18]. The free unprotected primary amine was converted into different guanidino groups upon reaction with the appropriate guanylating agent, following modified procedures already reported [22–24]. The conjugates $\mathbf{L^1}$ and $\mathbf{L^3}$ were prepared by reacting **pzC$_3$NH$_2$NH-Boc** with 1*H*-pyrazole-1-carboximidamide or *N*-methyl-1*H*-pyrazole-1-carboximidamide, respectively, followed by Boc-deprotection with trifluoroacteic acid (TFA) [22]. $\mathbf{L^2}$ was synthesized by reaction of the same precursor with cyanogen bromide, followed by hydroxyguanylation with hydroxylamine, and removal of the Boc-protecting group with TFA [23]. The synthesis of $\mathbf{L^4}$, which bears a pendant *N*-nitroguanidine group, was accomplished by nitroguanylation of the precursor compound with 2-methyl-1-nitro-2-thiopseudourea [24]. The S-methylisothiourea-containing conjugate $\mathbf{L^5}$ was obtained as a side product in the preparation of $\mathbf{L^4}$.

Conjugates $\mathbf{L^1}$–$\mathbf{L^5}$ were purified by semi-preparative RP-HPLC (>95% purity) and thoroughly characterized by multinuclear NMR (^{1}H, ^{13}C, g-COSY, g-HSQC) and IR spectroscopy, and ESI-MS. Besides the resonances due to the methylenic protons of the ligand backbone, the ^{1}H NMR spectra (D$_2$O) of the conjugates presented the typical sharp singlet peaks for the H(4) of the pyrazolyl ring and the methyl groups of the same ring. Singlet peaks for the *N*-methylguanidine ($\mathbf{L^3}$) and S-methylisothiourea ($\mathbf{L^5}$) groups were also found at δ 2.65 and δ 2.44, respectively. The ^{13}C spectra presented signals corresponding to all the expected carbon nuclei of the molecules.

2.2. Synthesis and characterization of complexes **1**/**1a**–**5**/**5a**

Reaction of $\mathbf{L^1}$–$\mathbf{L^5}$ with the organometallic precursors *fac*-[M(CO)$_3$(H$_2$O)$_3$]$^+$ afforded cationic complexes of the type *fac*-[M(CO)$_3$(k^3-L)]$^+$ (M = Re/^{99m}Tc; **1**/**1a**, L = $\mathbf{L^1}$; **2**/**2a**, L = $\mathbf{L^2}$; **3**/**3a**, L = $\mathbf{L^3}$; **4**/**4a**, L = $\mathbf{L^4}$; **5**/**5a**, L = $\mathbf{L^5}$) under the conditions depicted in Scheme 2.

The rhenium complexes **1**–**5**, synthesized and fully characterized as "cold" surrogates of the analog radioactive complexes **1a**–**5a**, were obtained in moderate yields (53%–80%) as air-stable viscous colorless oils after purification by RP-HPLC (>95% purity). Complexes **1**–**5** were characterized by RP-HPLC, ESI-MS and NMR spectroscopy (^{1}H/^{13}C NMR, ^{1}H–^{1}H COSY, and ^{1}H–^{13}C HSQC), and X-ray diffraction analysis in the case of complex **1**.

The ^{1}H NMR spectra (D$_2$O) of all complexes displayed the singlet peaks attributed to the H(4) and methyl groups of the pyrazolyl ring. The chemical shifts and splitting pattern of the diastereotopic amine protons and methylenic protons of the coordinating conjugates are comparable to those found for other complexes of the same type previously described by our group [14,15,17]. To illustrate such behavior, the fully assigned ^{1}H NMR spectrum of complex **3** is presented in the supplementary information (Fig. S1).

The ^{13}C spectra of **1**–**5** displayed also the expected signals for all carbon nuclei.

The NMR data obtained for all complexes is consistent with the expected tridentate coordination mode of the pyrazolyl-diamine chelating unit (*N*,*N*,*N* donor atom set) in conjugates $\mathbf{L^1}$–$\mathbf{L^5}$. This structure was confirmed by X-ray structure analysis of complex **1** (Fig. 2).

2.2.1. Crystal structure determination of the complex **1**

Suitable crystals of *fac*-[Re(CO)$_3$(k^3-$\mathbf{L^1}$)]·[TFA]$_2$ (**1**·[TFA]$_2$) were grown by slow evaporation of a MeOH/CH$_2$Cl$_2$ solution of the rhenium complex. A summary of the crystal data, structure solution

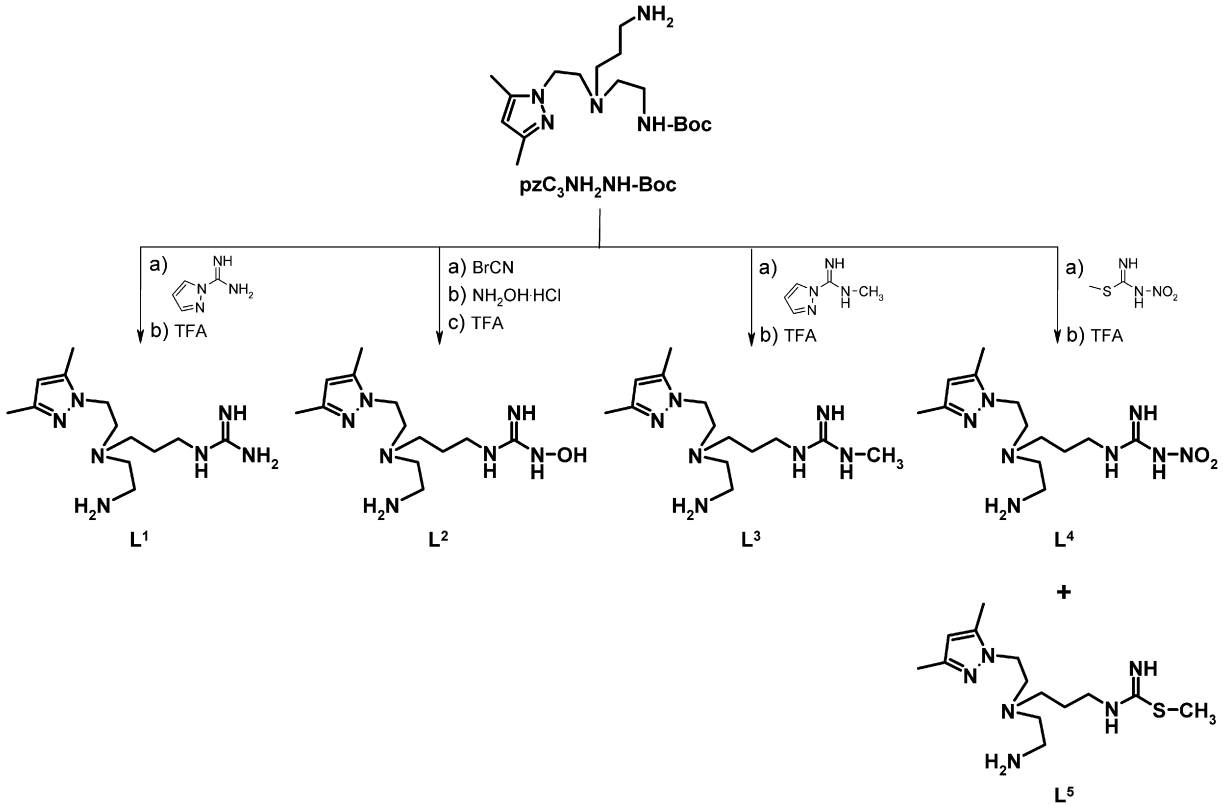

Scheme 1. Synthesis of the novel conjugates $\mathbf{L^1}$–$\mathbf{L^5}$.

and refinement parameters are given in Table 2 (Experimental section). An ORTEP diagram of $\mathbf{1}\cdot[TFA]_2$, together with selected bond lengths and angles are given in Fig. 2.

The Re atom in the complex is six-coordinated, being one of the triangular faces of the octahedron defined by three carbonyl ligands and the other by the nitrogen atoms of the pyrazolyl-diamine chelating unit. The Re–C and Re–N bond distances and angles can be considered unexceptional and are within the range found for other tricarbonyl complexes stabilized by ligands containing the tridentate pyrazolyl-diamine chelating unit [14,15].

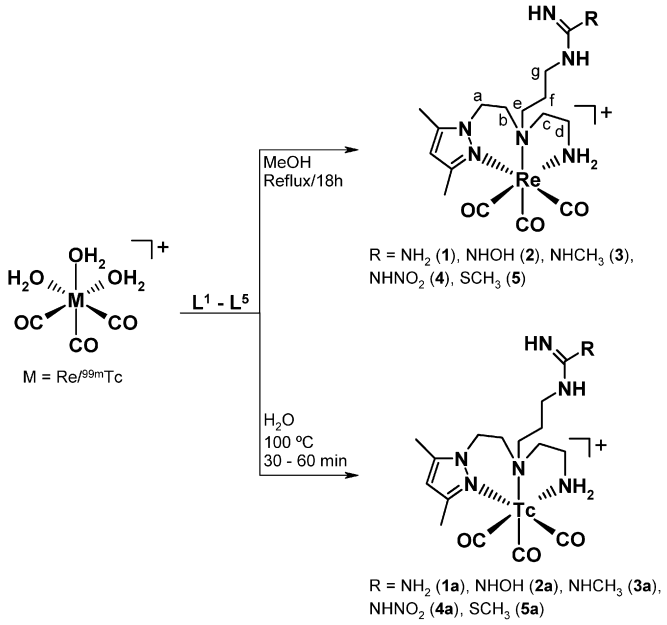

Scheme 2. Synthesis of the M(I)-tricarbonyl complexes **1**/**1a**–**5**/**5a**. *Identification system for NMR assignments is displayed.*

2.2.2. Characterization of the radioactive complexes *1a*–*5a*

The single well-defined radioactive complexes *fac*-[^{99m}Tc$(CO)_3(k^3$-L)]$^+$ (**1a**, L = $\mathbf{L^1}$; **2a**, L = $\mathbf{L^2}$; **3a**, L = $\mathbf{L^3}$; **4a**, L = $\mathbf{L^4}$; **5a**, L = $\mathbf{L^5}$), obtained in high yield and high radiochemical purity (>95%), were identified and characterized by RP-HPLC, comparing their γ-traces with the UV–Vis traces of the corresponding rhenium surrogates **1**–**5**. As an illustrative example, we present the RP-HPLC profiles of complexes **4** and **4a** in the supplementary information (Fig. S2).

The hydro(lipo)philic nature of the ^{99m}Tc(I)-complexes was evaluated by determining the partition coefficient (log $P_{o/w}$) in physiological conditions following a described procedure [25]. The results found were: log $P_{o/w} = -1.23 \pm 0.15$ (**1a**), -0.73 ± 0.10 (**2a**), -0.89 ± 0.20 (**3a**), -0.85 ± 0.22 (**4a**), and -0.05 ± 0.12 (**5a**). Analysis of the data has shown that complexes **1a**, **3a**, and **4a** displayed the highest hydrophilic nature, while complex **5a** is the most lipophilic complex.

The *in vitro* stability studies performed (incubation with solutions of histidine, cysteine, and phosphate-buffered saline pH 7.4, at 37 °C for 18 h) demonstrated that all ^{99m}Tc(I)-complexes are stable, since no peaks assigned to decomposition or reoxidation products were observed in the RP-HPLC chromatograms (purity ≥ 95%). Indeed, only the peak corresponding to the complex could be found.

2.3. Assay of iNOS activity in vitro

The new conjugates and the corresponding rhenium complexes were tested as NO-producing substrates ($\mathbf{L^1}$, $\mathbf{L^2}$, **1** and **2**) or

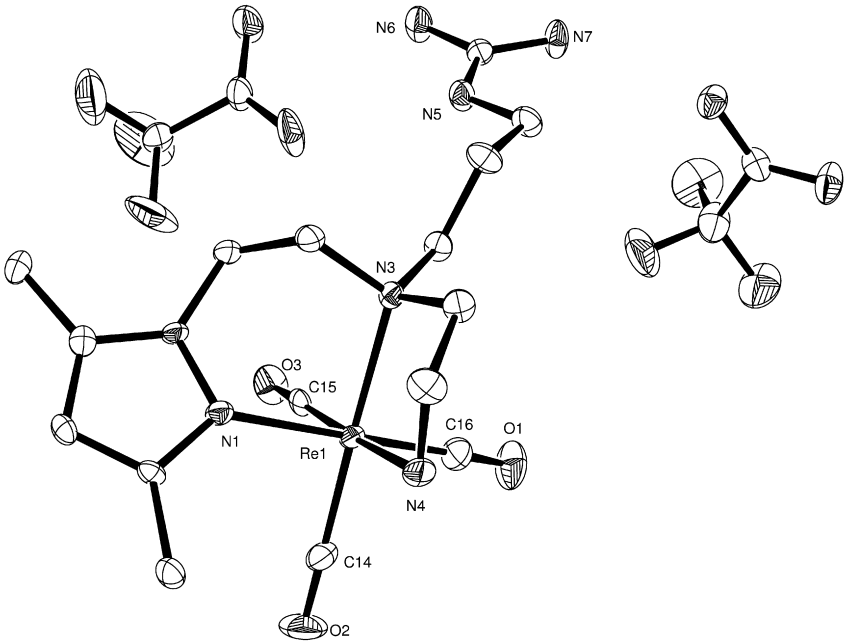

Fig. 2. ORTEP view of **1**·[TFA]$_2$. The hydrogen atoms are omitted for clarity. Vibrational ellipsoids are drawn at the 50% probability level. Selected bond distances (Å) and angles (°): Re–C14, 1.907(5) Å; Re–C15, 1.909(5) Å; Re–C16, 1.925(5) Å; Re–N1, 2.210(4) Å; Re–N3, 2.286(4) Å; Re–N4, 2.220(4) Å; C14–Re–N1, 93.6(18)°; C15–Re–N1, 90.1(17)°; C14–Re–N3, 174.2(19)°; C16–Re–N3, 95.9(18)°; C16–Re–N4, 95.0(2)°; C14–Re–C15, 86.5(2)°; C14–Re–C16, 86.0(2)°; N1–Re–N3, 84.9(14)°; N1–Re–N4, 89.3(15)°.

competitive inhibitors (**L^3**–**L^5** and **3**–**5**) on purified mouse recombinant iNOS. The iNOS activity was determined spectrophotometrically by monitoring the NO-mediated conversion of oxyhemoglobin to methemoglobin at 401 nm and 421 nm (see Experimental Section). The kinetic parameters K_m and K_i, determined by the method of Eisenthal and Cornish-Bowden, are summarized in Table 1.

The ability of **L^1** (K_m = 553 μM) and **L^2** (K_m = 1675 μM), which contain a guanidine or *N*-hydroxyguanidine moiety, respectively, to interact with the active site of iNOS leading to NO production, is negligible compared to the natural substrate of the enzyme (L-arginine, K_m = 6 μM). Metallation of **L^1** and **L^2** led to complexes with lower (**1**, K_m = 1035 μM) or comparable (**2**, K_m = 1465 μM) NO-producing properties, respectively. These results suggest that the presence of an α-amino-acid function in the compounds is a key issue for interaction with the enzyme active site and, consequently, has a decisive influence on their NO-producing properties.

Table 1
K_m and K_i values for the conjugates **L^1**–**L^5** and Re(I)-complexes **1**–**5**.

Compound	K_m values/μM[a]
L-Arginine	6 [17,26]
L^1	553
fac-[Re(CO)$_3$(k^3-**L^1**)] (**1**)	1035
L^2	1675
fac-[Re(CO)$_3$(k^3-**L^2**)] (**2**)	1465
Compound	K_i values/μM[a]
N$^{(\omega)}$–NO$_2$-L-arginine	3–8 [17,27]
N$^{(\omega)}$–CH$_3$-L-arginine	4–8 [17,27]
L^3	413
fac-[Re(CO)$_3$(k^3–**L^3**)] (**3**)	454
L^4	1087
fac-[Re(CO)$_3$(k^3–**L^4**)] (**4**)	257
L^5	1019
fac-[Re(CO)$_3$(k^3–**L^5**)] (**5**)	183

[a] Results are given as a mean of three or more independent experiments. Standard deviations of ± 5–10% were observed.

The inhibitory potency of the conjugates **L^3**–**L^5** is significantly lower (**L^3** K_i = 413 μM, **L^4** K_i = 1087 μM, and **L^5** K_i = 1019 μM) than that observed for the inhibitors N$^{(\omega)}$-NO$_2$-L-arginine (K_i = 3–8 μM) and N$^{(\omega)}$-CH$_3$-L-arginine (K_i = 4–8 μM), and analog conjugates with pendant L-arginine derivatives (K_i = 18–178 μM) described by our group [17]. Reaction of the conjugates **L^3**–**L^5** with the organometallic core *fac*-[Re(CO)$_3$]$^+$ yielded complexes with similar(**3**, K_i = 454 μM) or increased inhibitory potencies (**4** K_i = 257 μM; **5**, K_i = 183 μM) toward the enzyme. This effect had been already observed in other Re(I)-biorganometallic complexes containing pendant inhibitors (N$^{(\omega)}$-NO$_2$-L-arginine and N$^{(\omega)}$-CH$_3$-L-arginine, Fig. 1) [17]. However, the latter complexes presented a higher inhibitory potency (K_i = 6–118 μM) than complexes **4**–**5**, which again indicates that the α-amino-acid function has a key role in the interaction between the complexes and the enzyme active site.

2.4. Assay of iNOS activity in vivo

Since crossing the cell membrane and subsequent interaction with the intracellular target (iNOS) is mandatory for tracer uptake and retention *in vivo*, we have tested the conjugates **L^3**–**L^5** and M(I)-complexes **3/3a**–**5/5a** (M = Re, ^{99m}Tc) in lipopolysaccharide (LPS)-activated RAW 264.7 macrophages. The *N*-(hydroxy)guanidine-containing compounds **L^1**, **L^2**, **1**, and **2** were not assayed in this cell model due to their low ability to recognize the iNOS active site, as demonstrated by the enzymatic assays.

RAW 264.7 macrophages were chosen because they produce high levels of NO due to iNOS overexpression after treatment with LPS [28]. iNOS overexpression was confirmed by western blot analysis of protein extracts using an anti-iNOS antibody [18].

We evaluated the ability of conjugates **L^3**–**L^5** and **3**–**5** to suppress NO biosynthesis by measuring nitrite accumulation in the culture media using the Griess reagent method (Fig. 3). To assess the intrinsic cytotoxicity of the compounds at the concentration used in the NO assay (500 μM) and, consequently, its influence in nitrite accumulation, we have also performed a cell viability assay

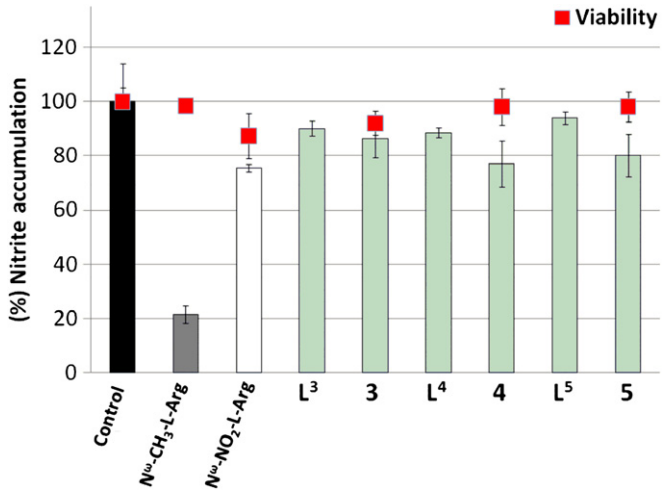

Fig. 3. Effect of compounds $\mathbf{L^3}$–$\mathbf{L^5}$ and **3**–**5** in nitrite accumulation, and cell viability in LPS-induced RAW 264.7 macrophages (mean ± S.D., $n = 8$). Final concentration of all compounds was 500 μM. NO production and viability in LPS-induced cells in the absence of any compound (control) was considered 100%. This experiment was repeated three times with comparable results.

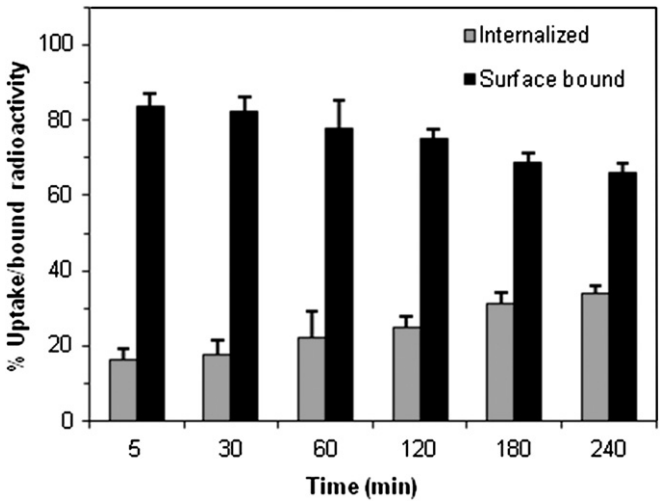

Fig. 4. Internalization of **4a** in LPS-induced RAW 264.7 macrophages (37 °C) at different time points (mean ± S.D., $n = 4$). Internalized and surface-bound activity expressed as a fraction of bound activity (activity on the membrane surface and inside the cell).

in parallel. These experiments have shown that all compounds are well tolerated by cells since no cytotoxic effects were observed under the described conditions (Fig. 3).

Analysis of the results has shown that all rhenium complexes were able to suppress NO production to a reasonable extent, being that effect more pronounced in the case of **4** and **5**, where ~20% NO suppression was observed. This value is comparable to that obtained for the inhibitor *N*ω-NO_2-L-arginine (*ca.* 20%), and correlates well with the *in vitro* enzymatic assays, where complexes **4** and **5** exhibited also the highest inhibitory potency towards iNOS (**4**, $K_i = 257$ μM; **5**, $K_i = 183$ μM).

Since the inhibition of NO biosynthesis is influenced not only by the intrinsic inhibitory capacity of the complexes, but also by their ability to cross cell membranes, we have also evaluated the internalization degree of the radioactive analog (**4a**) of the best performing rhenium complex (**4**) in LPS-activated RAW 264.7 macrophages. These studies have shown that the cellular uptake was time-dependent (Fig. 4). The highest level of internalization was reached at 4 h post-incubation, when 33.8% of the total cell-associated radioactivity for the applied radioconjugate was taken up and internalized by the cells, corresponding to 0.4% of the total activity applied.

Brought together, the NO suppression assays and internalization studies in LPS-activated macrophages have shown that Re(I)/^{99m}Tc (I) complexes with pendant amidinic moieties, where the α-amino-acid function is absent, cross cell membranes and interact specifically with iNOS. Indeed, the matched pair **4/4a** is a rare example of organometallic complexes able to cross cell membranes and interact specifically with a cytosolic enzyme.

3. Conclusions

We have synthesized a novel family of complexes of the type *fac*-$[M(CO)_3(k^3\text{-}L)]^+$ (M = Re/^{99m}Tc; **1**/**1a**, L = $\mathbf{L^1}$; **2**/**2a**, L = $\mathbf{L^2}$; **3**/**3a**, L = $\mathbf{L^3}$; **4**/**4a**, L = $\mathbf{L^4}$; **5**/**5a**, L = $\mathbf{L^5}$) stabilized by conjugates containing pendant guanidino ($\mathbf{L^1}$: guanidine, $\mathbf{L^2}$: *N*-hydroxyguanidine, $\mathbf{L^3}$: *N*-methylguanidine, $\mathbf{L^4}$: *N*-nitroguanidine) or S-methylisothiourea ($\mathbf{L^5}$) groups for iNOS recognition. Enzymatic assays with murine purified iNOS have shown that metallation of $\mathbf{L^3}$–$\mathbf{L^5}$ yielded complexes with similar (**3**, $K_i = 454$ μM) or increased inhibitory potencies (**4** $K_i = 257$ μM; **5**, $K_i = 183$ μM) toward the enzyme. The organometallic complexes **3/3a**–**5/5a** permeate through RAW 264.7 macrophage cell membranes, interacting specifically with the target cytosolic enzyme, as confirmed by the partial suppression of NO biosynthesis in LPS-treated macrophages and internalization studies. The results presented herein have shown that ^{99m}Tc(I)/Re (I) complexes with pendant *N*-nitroguanidine (**4**/**4a**) or S-methyl-isothiourea (**5**/**5a**) moieties may hold potential for targeting iNOS expression *in vivo*, despite their lower ability to interact with the enzyme, when compared with analog complexes containing the α-amino-acid function.

4. Experimental

4.1. General

All chemicals and solvents were of reagent grade and were used without purification unless stated otherwise. The precursor *tert*-butyl 2-((3-aminopropyl)(2-(3,5-dimethyl-1*H*-pyrazol-1-yl)ethyl)amino)ethylcarbamate (**pzC$_3$NH$_2$NH-Boc**) and [Re$(CO)_3(H_2O)$]Br were prepared according to published methods [18,29]. All other chemicals were purchased from Aldrich. Na[$^{99m}TcO_4$] was eluted from a ^{99}Mo/^{99m}Tc generator using 0.9% saline. The radioactive precursor *fac*-[^{99m}Tc$(CO)_3(H_2O)_3]^+$ was prepared using a IsoLink® kit (Malinckrodt-Covidean, Inc.). ^{1}H and ^{13}C-NMR spectra were recorded at room temperature on a Varian Unity 300 MHz spectrometer. ^{1}H and ^{13}C chemical shifts were referenced with the residual solvent resonances relatively to tetramethylsilane. The spectra were assigned with the help of 2D experiments (^{1}H–^{1}H correlation spectroscopy, COSY and ^{1}H–^{13}C heteronuclear single quantum coherence, HSQC). Assignments of the ^{1}H and ^{13}C-NMR resonances are given in accordance with the identification system shown in Scheme 2. All compounds were characterized by electrospray ionization mass spectrometry (ESI-MS) using a Bruker model Esquire 3000 plus. Aliquots of ~5 mg of pure compounds (≥95% ascertained by RP-HPLC) were lyophilized in eppendorf tubes and used for radioactive labelling and *in vitro* studies. HPLC analyses were performed on a Perkin Elmer LC pump 200 coupled to a Shimadzu SPD 10AV UV/Vis and to a Berthold-LB 509 radiometric detector, using an analytical

Table 2
Crystallographic data of the rhenium complex **1**·$[TFA]_2$.

Empirical formula	$C_{20}H_{28}F_6N_7O_7Re$
Formula weight	778.69
Diffractometer	Bruker-AXS APEX
Wavelength	0.71073 Å
Crystal system	Monoclinic
Space group	P21/n
Unit cell dimensions	a = 8.9966(3) Å b = 7.4433(2) Å c = 40.7831(11) Å β = 95.568(2)°
Volume	2718.13(14) Å^3
Z	4
Density (calculated)	1.903 Mg/m^3
Absorption coefficient	4.565 mm^{-1}
F(000)	1528
Crystal size	0.28 × 0.18 × 0.10 mm^3
θ range	3.12–25.03°
Index ranges	$-10 \le h \le 10$, $-8 \le k \le 8$, $-48 \le l \le 47$
Reflections collected	18137
Independent reflections	4781 [R(int) = 0.0325]
Completeness to θ	99.6% (25.03°)
Max. and min. transmission	0.6582 and 0.3613
Data/restraints/parameters	4781/0/372
Goodness-of-fit on F^2	1.260
Final R indices [I > 2sigma(I)]	R_1 = 0.0327, wR_2 = 0.0654
R indices (all data)	R1 = 0.0350, wR2 = 0.0662
Largest diff. peak and hole	1.163 and −1.984 e Å^{-3}

Macherey-Nagel C18 reversed-phase column (Nucleosil 100-5, 250 × 3 mm) with a flow rate of 0.5 ml/min. Purification of the inactive compounds were achieved on a semi-preparative Macherey-Nagel C18 reversed-phase column (Nucleosil 100-7, 250 × 8 mm) or on a preparative Waters μ Bondapak C18 (150 × 19 mm) with a flow rate of 2.0 ml/min and 5.5 ml/min, respectively. UV detection: 220 nm. Eluents: A = aqueous 0.1% CF_3COOH and B = MeOH. Gradient: t = 0–3 min, 0% B; 3–3.1 min, 0 → 25% B; 3.1–9 min, 25% B; 9–9.1 min, 25 → 34% B; 9.1–20 min, 34 → 100% B; 20–25 min, 100% B; 25–25.1 min, 100 → 0% B; 25.1–30 min, 0% B.

NOS assays were recorded on an Agilent Technologies 8453 UV–Vis diode array spectrophotometer with a thermostated multicuvette holder with stirring. The iNOS (mouse recombinant enzyme), bovine hemoglobin, NADPH, BH_4 (Tetrahydrobiopterin), HEPES and DTT were purchased from Sigma Chemical Co.

4.2. Synthetic procedures

4.2.1. Synthesis of conjugates L^1–L^5

4.2.1.1. 1-(3-((2-aminoethyl)(2-(3,5-dimethyl-1H-pyrazol-1-yl)ethyl) amino)propyl)guanidine (L^1). To a solution of **pzC$_3$NH$_2$NH-Boc** (190 mg, 0.559 mmol) in DMF was added 1*H*-pyrazole-1-carboxamidine hydrochloride (114 mg, 0.783 mmol), and DIPEA (101 mg, 0.783 mmol) in the same solvent. After stirring at room temperature for 18 h the solvent was evaporated and the crude product purified by silica-gel column chromatography ($CHCl_3$ to MeOH) to give **L^{1}Boc** as a pale yellow oil. **L^1** was obtained directly by Boc-deprotection of **L^{1}Boc** with a TFA/CH_2Cl_2 solution (1:1.4 ml) at room temperature for 3 h. The solvent was evaporated and the obtained residue dissolved in water and purified by RP-HPLC to give a colorless oil. Overall yield: 21.1% (60 mg, 0.118 mmol, calcd. for $C_{13}H_{27}N_7 \cdot 2TFA$). ^{1}H NMR ($D_2O$): δ(ppm) 6.13 (s, pz, 1H), 4.50 (t, CH_2, 2H), 3.53 (t, CH_2, 2H), 3.43 (m, CH_2, 2H), 3.29 (m, CH_2, 2H), 3.11 (m, CH_2, 4H), 2.20 (s, CH_3pz, 3H), 2.14 (s, CH_3pz, 3H), 1.83 (m, CH_2, 2H). ^{13}C NMR (D_2O): δ(ppm) 162.3 (q, CF_3COO^-), 156.1 (C=N), 147.3 (pz), 145.6 (pz), 115.5 (q, CF_3COO^-), 107.4 (pz), 50.5, 50.3, 49.0, 41.5, 37.2, 32.9, 22.0, 9.9 (CH_3pz), 9.4 (CH_3pz). ESI-MS (+) (*m*/*z*): 282.1 $[M + H]^+$; calcd for $C_{13}H_{27}N_7$ = 281.2. Retention time (analytical RP-HPLC, 220 nm): 13.8 min.

4.2.1.2. 1-(3-((2-aminoethyl)(2-(3,5-dimethyl-1H-pyrazol-1-yl) ethyl)amino)propyl)-3-hydroxy-guanidine (L^2). To a solution of **pzC$_3$NH$_2$NH-Boc** (90 mg, 0.265 mmol) and NEt_3 (40 mg, 0.397 mmol) in dry CH_2Cl_2, BrCN (84 mg, 0.795 mmol) dissolved in dry CH_2Cl_2 was added dropwise at 0 °C, under stirring, which was continued at room temperature overnight. Excess BrCN (56 mg, 0.530 mmol) was added at 0 °C to force reaction to completion. After 4 h, the solvent was evaporated and the crude cyanamide purified by column chromatography (EtOAc to MeOH) to give a pale yellow oil. Yield: 61.9% (60 mg, 0.144 mmol). ^{1}H NMR ($CDCl_3$): δ (ppm) 5.77 (s, pz, 1H), 5.65 (br s, NH, 1H), 5.34 (br s, NH, 1H), 4.08 (t, CH_2, 2H), 3.52 (m, CH_2, 2H), 3.11 (m, CH_2, 2H), 2.89 (m, CH_2, 2H), 2.58 (m, CH_2, 4H), 2.21 (s, CH_3pz, 3H), 2.18 (s, CH_3pz, 3H), 1.87 (m, CH_2, 2H), 1.40 (s, CH_3, 9H). ^{13}C NMR ($CDCl_3$): δ(ppm) 158.9 (CO), 157.0 (cyanamide), 147.6 (pz), 131.1 (pz), 105.6 (pz), 79.3 ($C(CH_3)_3$), 53.6, 52.9, 51.1, 45.8, 38.1, 37.5, 28.2 ($C(CH_3)_3$), 24.8, 13.1 (CH_3pz), 10.8 (CH_3pz). A mixture of the purified cyanamide (60 mg, 0.144 mmol), K_2CO_3 (23 mg, 0.330 mmol), and $H_2NOH.HCl$ (46 mg, 0.330 mmol) in anhydrous EtOH was stirred at room temperature for 18 h. The solution was then filtered to remove an insoluble white solid. After evaporation of the filtrate, the residue was purified by silica-gel column chromatography (CH_2Cl_2 to MeOH). Evaporation of the solvent from the collected fractions yielded **L^{2}Boc** as a colorless oil. Yield: 46.0% (30 mg, 0.076 mmol). Compound **L^2** was prepared by using the standard TFA Boc-deprotection conditions described above. Starting from 30 mg (0.076 mmol) of **L^{2}Boc**, a colorless oil formulated as **L^2** was obtained after purification by RP-HPLC. Yield: 70.3% (22 mg, 0.053 mmol, calcd. for $C_{13}H_{27}N_7O \cdot TFA$). ^{1}H NMR ($D_2O$): δ(ppm) 5.98 (s, pz, 1H), 4.33 (t, CH_2, 2H), 3.48 (t, CH_2, 2H), 3.37 (m, CH_2, 2H), 3.28 (m, CH_2, 2H), 3.15 (m, CH_2, 2H), 3.03 (m, CH_2, 2H), 2.17 (s, CH_3pz, 3H), 2.09 (s, CH_3pz, 3H), 1.79 (m, CH_2, 2H). ^{13}C NMR (D_2O): δ(ppm) 165.4 (q, CF_3COO^-), 156.1 (C=N), 151.2 (pz), 144.3 (pz), 118.5 (q, CF_3COO^-), 108.2 (pz), 54.6, 53.0, 52.6, 47.4, 41.1, 38.7, 27.0, 14.4 (CH_3pz), 12.5 (CH_3pz). ESI-MS (+) (*m*/*z*): 298.1 $[M + H]^+$; calcd for $C_{13}H_{27}N_7O$ = 297.2. Retention time (analytical RP-HPLC, 220 nm): 14.2min.

4.2.1.3. 1-(3-((2-aminoethyl)(2-(3,5-dimethyl-1H-pyrazol-1-yl) ethyl)amino)propyl)-3-methyl-guanidine (L^3). Method A: *N*-methyl-1*H*-pyrazole-1-carboximidamide (47 mg, 0.294 mmol), prepared as described in supplementary information, and **pzC$_3$NH$_2$NH-Boc** (50 mg, 0.147 mmol) were mixed in water (pH 2 to 3). The pH of the solution was adjusted to 10–11 with lithium hydroxide monohydrate (18 mg, 0.441 mmol). After stirring for 2 days at room temperature, 1 equivalent of *N*-methyl-1*H*-pyrazole-1-carboximidamide was added and stirring continued for more 3 days. The solvent was removed, the residue dissolved in CH_2Cl_2, filtered, and applied on a silica-gel column, which was eluted with CH_2Cl_2–MeOH (gradient). Removal of the solvent from the collected fractions gave **L^{3}Boc**. Yield: 51.6% (30 mg, 0.076 mmol).

Method B: **L^{3}Boc** was prepared by using the same reaction conditions described above for **L^{1}Boc** (Section 4.2.1.1.). Starting from 50 mg (0.147 mmol) of **pzC$_3$NH$_2$NH-Boc**, 47 mg of *N*-methyl-1*H*-pyrazole-1-carboximidamide (0.294 mmol), and 37 mg of DIPEA (0.294 mmol) in DMF, **L^{3}Boc** was obtained as a yellow pale oil after purification by column chromatography (CH_2Cl_2 to MeOH). Yield: 48.1% (28 mg, 0.070 mmol).

L³Boc (30 mg, 0.076 mmol) was dissolved in a mixture of TFA (2 ml) and CH_2Cl_2 (1:1) and stirred at room temperature for 3 h. **L³** was obtained as colorless oil after purification by RP-HPLC. Yield: 73.9% (23 mg, 0.056 mmol, calcd. for $C_{14}H_{29}N_7 \cdot TFA$). ^1H NMR (D_2O): δ(ppm) 6.01 (s, pz, 1H), 4.38 (t, CH_2, 2H), 3.53 (t, CH_2, 2H), 3.51 (m, CH_2, 2H), 3.38 (m, CH_2, 2H), 3.27 (m, CH_2, 2H), 3.03 (m, CH_2, 2H), 2.65 (s, C–NH–CH_3, 3H), 2.15 (s, CH_3pz, 3H), 2.08 (s, CH_3pz, 3H), 1.79 (m, CH_2, 2H). ^{13}C NMR (D_2O): δ(ppm) 165.3 (q, CF_3COO^-), 162.6 (C=N), 155.7 (pz), 148.4 (pz), 115.6 (q, CF_3COO^-), 106.1 (pz), 51.4, 50.6, 49.2, 42.0, 37.3, 33.3, 26.6, 22.4, 11.0 (CH_3pz), 9.3 (CH_3pz). ESI-MS (+) (*m*/*z*): 296.1 $[M + H]^+$; calcd for $C_{14}H_{29}N_7$ = 295.2. Retention time (analytical RP-HPLC, 220 nm): 15.0 min.

*4.2.1.4. 1-(3-((2-aminoethyl)(2-(3,5-dimethyl-1H-pyrazol-1-yl)ethyl) amino)propyl)-3-nitro-guanidine (**L⁴**) and methyl 3-((2-aminoethyl) (2-(3,5-dimethyl-1H-pyrazol-1-yl)ethyl)amino)propylcarbamimidothioate (**L⁵**).* To a stirred solution of **pzC₃NH₂NH-Boc** (80 mg, 0.235 mmol) in anhydrous EtOH were added NEt_3 (145 mg, 1.41 mmol) and 2-methyl-1-nitro-2-thiopseudourea (95 mg, 0.706 mmol) prepared as described in supplementary material. The reaction temperature was then raised to 40 °C, and stirring continued overnight under nitrogen. The solvent was evaporated under reduced pressure, and the crude residue was purified by a silica-gel column (CH_2Cl_2 to MeOH), giving **L⁴Boc** (55 mg, 0.128 mmol, 54.9%) and **L⁵Boc** (22 mg, 0.053 mmol, 22.7%) as pure compounds. Boc-deprotection of **L⁴Boc** (35 mg, 0.082 mmol) and **L⁵Boc** (20 mg, 0.048 mmol) with TFA, followed by RP-HPLC purification gave **L⁴** (30 mg, 0.068 mmol, 83.0%, calcd. for $C_{13}H_{26}N_8O_2 \cdot TFA$) and **L⁵** (16 mg, 0.037 mmol, 78.1%, calcd. for $C_{14}H_{29}N_7S \cdot TFA$), respectively.

L⁴: IR (KBr, cm^{-1}): 1711m, 1314w (NO_2), 1213m, 1123m, 837w, 800w and 723w. ^1H NMR (D_2O): δ(ppm) 6.03 (s, pz, 1H), 4.42 (t, CH_2, 2H), 3.56 (t, CH_2, 2H), 3.46 (m, CH_2, 2H), 3.32 (m, CH_2, 2H), 3.18 (t, CH_2, 2H), 3.09 (m, CH_2, 2H), 2.17 (s, CH_3pz, 3H), 2.10 (s, CH_3pz, 3H), 1.84 (m, CH_2, 2H). ^{13}C NMR (D_2O): δ(ppm) 162.9 (q, CF_3COO^-), 158.3 (C=N), 147.9 (pz), 144.2 (pz), 115.4 (q, CF_3COO^-), 106.7 (pz), 50.6, 49.1, 41.6, 37.1, 33.0, 22.3, 22.0, 10.4 (CH_3pz), 9.3 (CH_3pz). ESI-MS (+) (*m*/*z*): 327.0 $[M + H]^+$; calcd for $C_{13}H_{26}N_8O_2$ = 326.2. Retention time (analytical RP-HPLC, 220 nm): 16.2 min.

L⁵: IR (KBr, cm^{-1}): 1703m, 1208m, 1127m, 839w and 801w. ^1H NMR (D_2O): δ(ppm) 5.85 (s, pz, 1H), 3.99 (t, CH_2, 2H), 3.07 (t, CH_2, 2H), 2.92 (m, CH_2, 2H), 2.86 (m, CH_2, 2H), 2.76 (m, CH_2, 2H), 2.48 (m, CH_2, 2H), 2.44 (s, SCH_3, 3H), 2.13 (s, CH_3pz, 3H), 2.07 (s, CH_3pz, 3H), 1.58 (m, CH_2, 2H). ^{13}C NMR (D_2O): δ(ppm) 168.2 (C=N), 147.9 (pz), 141.0 (pz), 104.9 (pz), 51.5, 49.8, 49.6, 44.9, 40.8, 36.0, 23.5, 12.5, 11.4 (CH_3pz), 9.4 (CH_3pz). ESI-MS (+) (*m*/*z*): 313.21 $[M + H]^+$; calcd for $C_{14}H_{28}N_6S$ = 312.21. Retention time (analytical RP-HPLC, 220 nm): 11.4 min.

*4.2.2. General procedure for the preparation of fac-[Re(CO)₃(k³-L)] (1, L = **L¹**; 2, L = **L²**; 3, L = **L³**; 4, L = **L⁴**; and 5, L = **L⁵**)*

$[Re(CO)_3(H_2O)_3]Br$ reacted with equimolar amounts of **L¹**–**L⁵** in refluxing MeOH for 18 h. The solvent was removed under vacuum, and the resulting residue dissolved in water and purified by preparative RP-HPLC.

*4.2.2.1. fac-[Re(CO)₃(k³-**L¹**)] (**1**).* Starting from 18 mg (0.035 mmol) of **L¹**·2TFA, a colorless oil formulated as **1** was obtained (22 mg, 80.6%, calcd. for $C_{16}H_{27}N_7O_3Re \cdot 2TFA$). ^1H NMR (CD_3OD): δ(ppm) 6.21 (s, pz(4), 1H), 5.57 (br s, NH, 1H), 4.50 (dd, CH^a, 1H), 4.22 (m, $CH^{a'}$, 1H), 4.10 (m, NH, 1H), 3.71 (m, CH^g, 1H), 3.47 (m, $CH^{g'}$ + CH^b, 2H), 3.20 (m, $CH^{e'}$ + CH^e, 2H), 3.14 (m, CH^d, 1H), 2.84 (m, $CH^{d'}$ + CH^c, 2H), 2.69 (m, $CH_2^{b'}$, 1H), 2.55 (m, $CH^{c'}$, 1H), 2.44 (s, CH_3pz, 3H), 2.36 (s, CH_3pz, 3H), 2.19 (m, CH_2^f, 1H), 2.17 (m, $CH_2^{f'}$, 1H). ^{13}C NMR (CD_3OD): δ(ppm) 197.3 (C≡O), 196.7 (C≡O), 195.5 (C≡O), 164.9 (q, CF_3COO^-), 158.5 (C=N), 156.5 (pz), 147.1 (pz), 118.0 (q, CF_3COO^-), 110.5 (pz), 65.7, 63.9, 55.4, 49.7, 44.9, 39.9, 25.2, 18.0 (CH_3pz), 13.6 (CH_3pz). ESI-MS (+) (*m*/*z*): 552.2 $[M]^+$, calcd. for $C_{16}H_{27}N_7O_3Re$ = 552.1. Retention time (analytical RP-HPLC, 220 nm): 19.0 min.

*4.2.2.2. fac-[Re(CO)₃(k³-**L²**)] (**2**).* Starting from 17 mg (0.041 mmol) of **L²**·TFA, a colorless oil formulated as **2** was obtained (15 mg, 53.7%, calcd. for $C_{16}H_{27}N_7O_4Re \cdot TFA$). ^1H NMR (D_2O): δ(ppm) 6.03 (s, pz(4), 1H), 5.07 (br s, NH, 1H), 4.28 (dd, CH^a, 1H), 4.06 (m, $CH^{a'}$, 1H), 3.64 (m, NH, 1H), 3.49 (m, CH^g, 1H), 3.35–3.23 (m, $CH^{g'}$ + CH^b, 2H), 3.20 (m, $CH^{e'}$ + CH^e, 2H), 3.07 (m, CH^d, 1H), 2.73 (m, $CH^{d'}$ + CH^c, 2H), 2.60 (m, $CH_2^{b'}$, 1H), 2.38 (m, $CH^{c'}$, 1H), 2.27 (s, CH_3pz, 3H), 2.15 (s, CH_3pz, 3H), 2.10 (m, CH_2^f, 1H), 1.91 (m, $CH_2^{f'}$, 1H). ^{13}C NMR (D_2O): δ(ppm) 193.8 (C≡O), 193.2 (C≡O), 192.0 (C≡O), 162.0 (q, CF_3COO^-), 158.0 (C=N), 152.9 (pz), 143.5 (pz), 115.0 (q, CF_3COO^-), 107.0 (pz), 63.6, 61.0, 52.4, 46.3, 41.4, 37.7, 23.4, 14.5 (CH_3pz), 10.0 (CH_3pz). ESI-MS (+) (*m*/*z*): 567.9 $[M]^+$, calcd. for $C_{16}H_{27}N_7O_4Re$ = 368.1. Retention time (analytical RP-HPLC, 220 nm): 19.1 min.

*4.2.2.3. fac-[Re(CO)₃(k³-**L³**)] (**3**).* Starting from 30 mg (0.073 mmol) of **L³**·TFA, a colorless oil formulated as **3** was obtained (35 mg, 70.5%, calcd. for $C_{17}H_{29}N_7O_3Re \cdot TFA$). ^1H NMR (D_2O): δ(ppm) 6.01 (s, pz(4), 1H), 5.06 (br s, NH, 1H), 4.32 (dd, CH^a, 1H), 4.02 (m, $CH^{a'}$, 1H), 3.63 (m, NH, 1H), 3.50 (m, CH^g, 1H), 3.39–3.26 (m, $CH^{g'}$ + CH^b, 2H), 3.18 (m, $CH^{e'}$ + CH^e, 2H), 3.02 (m, CH^d, 1H), 2.71 (m, $CH^{d'}$ + CH^c, 2H), 2.66 (s, C–NH–CH_3, 3H), 2.57 (m, $CH_2^{b'}$, 1H), 2.36 (m, $CH^{c'}$, 1H), 2.26 (s, CH_3pz, 3H), 2.16 (s, CH_3pz, 3H), 2.06 (m, CH_2^f, 1H), 1.87 (m, $CH_2^{f'}$, 1H). ^{13}C NMR (D_2O): δ(ppm) 193.7 (C≡O), 193.3 (C≡O), 192.0 (C≡O), 162.4 (q, CF_3COO^-), 161.9 (C=N), 155.7 (pz), 152.9 (pz), 115.3 (q, CF_3COO^-), 107.0 (pz), 63.7, 61.1, 52.5, 46.4, 41.4, 37.7, 26.7, 23.6, 14.5 (CH_3pz), 10.1 (CH_3pz). ESI-MS (+) (*m*/*z*): 566.0 $[M]^+$, calcd. for $C_{17}H_{29}N_7O_3Re$ = 566.1. Retention time (analytical RP-HPLC, 220 nm): 19.2 min.

*4.2.2.4. fac-[Re(CO)₃(k³-**L⁴**)] (**4**).* Starting from 20 mg (0.045 mmol) of **L⁴**·TFA, a colorless oil formulated as **4** was obtained (25 mg, 78.2%, calcd. for $C_{16}H_{26}N_8O_5Re \cdot TFA$). ^1H NMR (CD_3OD): δ(ppm) 5.99 (s, pz(4), 1H), 5.35 (br s, NH, 1H), 4.32–4.23 (dd, CH^a, 1H), 4.07–4.00 (m, $CH^{a'}$, 1H), 3.63 (m, NH, 1H), 3.48 (m, CH^g, 1H), 3.36–3.20 (m, $CH^{g'}$ + CH^b, 2H), 3.20–3.10 (m, $CH^{e'}$ + CH^e, 2H), 3.00 (m, CH^d, 1H), 2.67 (m, $CH^{d'}$ + CH^c, 2H), 2.54 (m, $CH_2^{b'}$, 1H), 2.32 (m, $CH^{c'}$, 1H), 2.22 (s, CH_3pz, 3H), 2.11 (s, CH_3pz, 3H), 2.10 (m, CH_2^f, 1H), 1.90 (m, $CH_2^{f'}$, 1H). ^{13}C NMR (CD_3OD): δ(ppm) 196.7 (C≡O), 196.2 (C≡O), 195.0 (C≡O), 161.4 (C=N), 155.9 (pz), 145.5 (pz), 110.1 (pz), 66.9, 64.0, 55.5, ~49.0 (overlapped with CD_3OD solvent peak), 44.4, 40.8, 26.0, 17.5, 13.1. ESI-MS (+) (*m*/*z*): 597.0 $[M]^+$, calcd. for $C_{26}H_{26}N_8O_5Re$ = 597.1. Retention time (analytical RP-HPLC, 220 nm): 19.9 min.

*4.2.2.5. fac-[Re(CO)₃(k³-**L⁵**)] (**5**).* Starting from 13 mg (0.030 mmol) of **L⁵**·TFA, a colorless oil formulated as **5** was obtained (35 mg, 73.3%, calcd. for $C_{17}H_{28}N_6O_3ReS \cdot TFA$). ^1H NMR (D_2O): δ(ppm) 6.04 (s, pz(4), 1H), 5.03 (br s, NH, 1H), 4.39 (dd, CH^a, 1H), 4.07 (m, $CH^{a'}$, 1H), 3.78 (m, NH, 1H), 3.54 (m, CH^g, 1H), 3.48–3.28 (m, $CH^{g'}$ + CH^b, 2H), 3.28–3.19 (m, $CH^{e'}$ + CH^e, 2H), 3.03 (m, CH^d, 1H), 2.74 (m, $CH^{d'}$ + CH^c, 2H), 2.59 (m, $CH_2^{b'}$, 1H), 2.45 (s, SCH_3, 3H), 2.37 (m, $CH^{c'}$, 1H), 2.27 (s, CH_3pz, 3H), 2.15 (s, CH_3pz, 3H), 2.14 (m, CH_2^f, 1H), 1.97 (m, $CH_2^{f'}$, 1H). ^{13}C NMR (D_2O): δ(ppm) 191.7 (C≡O), 191.2 (C≡O), 189.9 (C≡O), 161.9 (C=N), 150.9 (pz), 141.4 (pz), 105.0 (pz), 61.4, 58.9, 50.3, 44.3, 39.4, 38.4, 21.4, 12.5, 10.4, 8.02. ESI-MS (+) (*m*/*z*): 583.0 $[M]^+$, calcd. for $C_{17}H_{28}N_6O_3SRe$ = 581.1. Retention time (analytical RP-HPLC, 220 nm): 19.6 min.

4.3. X-ray crystallographic analysis

A colorless crystal of **1**·$[TFA]_2$, suitable for X-ray diffraction analysis, was obtained by slow evaporation of a $MeOH/CH_2Cl_2$ solution of the compound obtained in Section 4.2.2.1 at room temperature. X-ray diffraction analysis has been performed on a Bruker AXS APEX CCD area detector diffractometer, using graphite monochromated Mo Ka radiation (0.71073 Å). Empirical absorption correction was carried out using SADABS [30]. Data collection and data reduction were done with the SMART and SAINT programs [31]. The structure was solved by direct methods with SIR97 [32] and refined by full-matrix least-squares analysis with SHELXL-97 [33] using the WINGX [34] suite of programmes. All non-hydrogen atoms were refined anisotropically. The remaining hydrogen atoms were placed in calculated positions. Molecular graphics were prepared using ORTEP3 [35]. A summary of the crystal data, structure solution and refinement parameters is given in Table 2, and selected bond lengths and angles appear in Fig. 2.

4.4. General procedure for the preparation of *fac*-[^{99m}Tc(CO)$_3$(k^3-L)] (1a, L = **L^1**; 2a, L = **L^2**; 3a, L = **L^3**; 4a, L = **L^4**; and 5a, L = **L^5**)

4.4.1. Preparation

In a nitrogen-purged glass vial, 100 μL of a 10^{-3} or 10^{-4} M aqueous solution of the corresponding conjugate (**L^1**–**L^4**) were added to 900 μL of a solution of the organometallic precursor *fac*-$[^{99m}Tc(H_2O)_3(CO)_3]^+$ (1–2 mCi) in saline. The reaction mixture was then heated to 100 °C for 30–60 min, cooled on an ice bath, and the final solution analyzed by RP-HPLC (labeling yield and radiochemical purity >95%). Retention times: 19.9 min (**1**), 20.1 min (**2**), 20.3 min (**3**), 20.2 min (**4**), and 20.7 min (**5**).

4.4.2. Stability - cysteine and histidine challenge

Aliquots of 100 μL of the ^{99m}Tc(I)-complexes were added to 400 μL of 5×10^{-3} M cysteine or histidine solutions in PBS (pH 7.4). The solutions were incubated at 37 °C for 24 h and analyzed by analytical RP-HPLC.

4.4.3. Partition coefficient

The lipophilicity of the radioconjugates was evaluated by the "shakeflask" method [25]. Briefly, the radioconjugates were added to a mixture of octanol (1 ml) and 0.1 M PBS pH = 7.4 (1 ml), previously saturated in each other by stirring the mixture. This mixture was vortexed and centrifuged (3000 rpm, 10 min, room temperature) to allow phase separation. Aliquots of both octanol and PBS were counted in a gamma counter. The partition coefficient ($P_{o/w}$) was calculated by dividing the counts in the octanol phase by those in the buffer, and the results expressed as Log $P_{o/w}$.

4.5. Enzyme kinetic assays

The iNOS activity assay was based on the hemoglobin assay previously described by Hevel and Marletta with slight modifications [26,36]. The kinetic parameters for iNOS were determined using initial rate analysis. Initial rate data were fitted to irreversible single substrate Michaelis–Menten models. The kinetic parameters were determined using the direct linear plot of Eisenthal and Cornish-Bowden and the Hyper software (J.S. Easterby, University of Liverpool, UK; http://www.liv.ac.uk/~jse/software.html) [37,38]. The K_m and K_i values represent a mean of triplicate measurements. Standard deviations of ±5–10% were observed.

4.5.1. Preparation of oxyhemoglobin

Oxyhemoglobin was prepared using a previously described protocol with some modifications [39]. Briefly, bovine hemoglobin in 50 mM HEPES pH 7.4 was reduced to oxyhemoglobin with 10-fold molar excess of sodium dithionite. The sodium dithionite was later removed by dialysis against 50 volumes of HEPES buffer for 18 h at 4 °C. The buffer was replaced 3 times. The concentration of oxyhemoglobin was determined spectrophotometrically using $\varepsilon_{415nm} = 131\ mM^{-1}\ cm^{-1}$. Oxyhemoglobin was stored at −80 °C before use.

4.5.2. Determination of kinetic parameters

4.5.2.1. Determination of K_m values. All initial velocity measurements were recorded at 37 °C. Total reaction volumes were 1500 μL and contained 50 mM HEPES pH 7.4, 6 μM oxyhemoglobin, 200 μM NADPH, 10 μM BH_4, 100 μM DTT and at least three concentrations of L-arginine, **L^1**, **L^2**, **1** and **2** (20–500 μM). Magnetic stirring in the spectrophotometer cuvette was essential to maintain isotropic conditions. Reactions were initiated by the addition of iNOS enzyme (~1 U) to the prewarmed cuvette (~5 min). The NO-mediated conversion of oxyhemoglobin to methemoglobin was followed by monitoring the increase in absorbance at dual wavelength (401 and 421 nm) for 10 min [40]. Controls were performed in the same conditions without iNOS enzyme.

4.5.2.2. Determination of K_i values. The K_i values were obtained by measuring inhibition with at least three concentrations of L-arginine (20–150 μM) in the presence of 150 μM of $N^{(\omega)}$-NO_2-L-arginine, $N^{(\omega)}$-Me-L-arginine, **L^3**, **L^4**, **L^5**, **3**, **4**, and **5** under the conditions previously described. The formula used to calculate the K_i is: $K_i = [I]/(K_m^{app}/K_m) - 1$ where [I] is the inhibitor concentration, K_m is the Michaelis–Menten constant of the substrate L-arginine and K_m^{app} is the apparent value of K_m for a substrate in the presence of the inhibitor [37]. K_m value for L-arginine was determined as 6 μM.

4.6. RAW 264.7 macrophages assay

4.6.1. Cell culture

RAW 264.7 macrophages were grown in Dulbecco's Modified Eagle Medium (DMEM) with GlutaMax I supplemented with 10% heat-inactivated fetal bovine serum and 1% penicillin/streptomycin antibiotic solution (all from Invitrogen, UK). Cells were cultured in a humidified atmosphere of 95% air and 5% CO_2 at 37 °C, with the medium changed every other day.

4.6.2. Evaluation of the inhibitory effect of the compounds in vivo

Macrophages (in DMEM without phenol red and 10% FBS) were plated at a density of 9×10^4 cells per well in 96-well plates. Cells were immediately induced with 10 μL of LPS (2 μg/ml in PBS) for 4 h, and then incubated for 24 h in the presence of the compounds (500 μM). At the end of the incubation period, the culture medium was collected and assayed for nitrite production using the commercially available Griess reagent method (Sigma–Aldrich) [41].

4.6.3. Cell viability assay

Cell viability was evaluated by using a colorimetric method based on the tetrazolium salt MTT ([3-(4,5-dimethylthiazol-2-yl)-2,5-diphenyltetrazolium bromide), which is reduced by viable cells to yield purple formazan crystals [42]. Cells were seeded in 96-well plates at a density of 9×10^4 cells per well, immediately induced with LPS (2 μg/ml) for 4h, and then incubated for 24 h in the presence of the compounds (500 μM). At the end of the incubation period the media was removed and the cells were incubated with MTT (0.5 mg/mL in culture medium; 200 μl) for 3–4 h at 37 °C and 5% CO_2. The purple formazan crystals formed inside the cells were then dissolved in 200 μl of DMSO by thorough shaking, and the absorbance was read at 570 nm, using a plate spectrophotometer (Power Wave Xs; Bio-Tek). Each test

was performed with at least six replicates and repeated at least 2 times. The result was expressed as percentage of the surviving cells in relation with the control.

4.7. Cellular internalization

Internalization assays were performed in RAW 264.7 macrophages seeded at a density of 0.3 million/well in complete culture medium containing LPS (2 μg/ml) in 24-well tissue culture for 24 h at 37 °C. Then, the culture medium was removed and cells were incubated with about 200000 cpm of the radiocomplex **4a** in 0.5 ml of assay medium (Modified Eagle's Medium with 25 mM HEPES and 0.2% BSA) for a period of 5 min–4 h at 37 °C. Incubation was terminated by washing the cells with ice-cold assay medium. Cell-surface bound radioligand was removed by two steps of acid wash (50 mM glycine·HCl/100 mM NaCl, pH 2.8) at room temperature for 5 min. The pH was neutralized with cold PBS with 0.2% BSA. The cells were then lysed by 10 min incubation with 0.5 N NaOH at 37 °C to determine internalized radioligand. The radioactivities of the lysates and cell-surface-bound fractions were counted in a γ-counter.

Acknowledgements

This work has been supported by the Fundação para a Ciência e Tecnologia (FCT), Portugal (POCI/SAU-FCF/58855/2004). B. L. Oliveira thanks FCT for a PhD grant (SFRH/BD/38753/2007). Dr. J. Marçalo is acknowledged for performing the ESI-MS analyses. The QITMS instrument was acquired with the support of Contract REDE/1503/REM/2005 - ITN) of FCT and is part of RNEM. Part of this work was supported by COST Action D39 "Metallo-drug design and action".

Appendix A. Supplementary material

CCDC number 790322 contains the supplementary crystallographic data for complex **1**·$[TFA]_2$. These data can be obtained free of charge from the Cambridge Crystallographic Data Centre via www.cdcc.cam.ac.uk/data_request/cif.

The supplementary material also includes the ^{1}H NMR spectrum of **3** (Fig. S1), RP-HPLC analytical chromatograms of **4**/**4a** (Fig. S2), and synthetic procedures for *N*-methyl-1*H*-pyrazole-1-carboximidamide and 2-methyl-1-nitro-2-thiopseudourea. These can be found in the online version at doi:10.1016/j.jorganchem.2010.09.019.

References

[1] S. Moncada, R.M.J. Palmer, E.A. Higgs, Pharmacol. Rev. 43 (1991) 109.
[2] J.F. Kerwin, J.R. Lancaster, J. Med. Chem. 38 (1995) 4343.
[3] M.A. Marletta, J. Biol. Chem. 268 (1993) 12231.
[4] W.K. Alderton, C.E. Cooper, R.G. Knowles, Biochem. J. 357 (2001) 593.
[5] Special issue on Nitric Oxide in Cancer Biology and Treatment, in: D.A. Wink, J.B. Mitchell (Eds.), Free Radic. Biol. Med., 34, 2003.
[6] D. Fukumura, S. Kashiwagi, R.K. Jain, Nat. Rev. Cancer 6 (2006) 521.
[7] A.J. Duncan, S.J. Heales, Mol. Aspects Med. 26 (2005) 67.
[8] H. Hong, J. Sun, W. Cai, Free Radic. Biol. Med. 47 (2009) 684.
[9] T. Nagano, T. Yoshimura, Chem. Rev. 102 (2002) 1235.
[10] J. Zhang, M. Xu, C.S. Dence, E.L.C. Sherman, T.J. MacCarthy, M.J. Welch, J. Nucl. Med. 38 (1997) 1273.
[11] D. Zhou, H. Lee, J.M. Rothfuss, D.L. Chen, D.E. Ponde, M.J. Welch, R.H. Mach, J. Med. Chem. 52 (2009) 2443.
[12] H.-J. Wester, Clin. Cancer Res. 13 (2007) 3470.
[13] L. Shuang, Adv. Drug Deliv. Rev. 60 (2008) 1347.
[14] J.D.G. Correia, A. Paulo, I. Santos, Curr. Radiopharm. 2 (2009) 277.
[15] I. Santos, A. Paulo, J.D.G. Correia, Top. Curr. Chem. 252 (2005) 45.
[16] P.D. Raposinho, J.D.G. Correia, M.C. Oliveira, I. Santos, Biopolymers (Pept Sci.) (2010). doi:10.1002/bip.21490.
[17] B.L. Oliveira, J.D.G. Correia, P.D. Raposinho, I. Santos, A. Ferreira, C. Cordeiro, A.P. Freire, Dalton Trans. (2009) 152.
[18] B.L. Oliveira, P.D. Raposinho, F. Mendes, F. Figueira, I. Santos, A. Ferreira, C. Cordeiro, A.P. Freire, J.D.G. Correia, Bioconjug Chem, in press.
[19] D. Mansuy, J.-L. Boucher, Free Radic. Biol. Med. 37 (2004) 1105.
[20] T.B. Cai, D. Lu, P.G. Wang, Curr. Top. Med. Chem. 5 (2005) 721.
[21] L. Salerno, V. Sorrenti, C. Di Giacomo, G. Romeo, M.A. Siracusa, Curr. Pharm. Des 8 (2002) 177.
[22] I. Gillies, Glaxo Group Limited, Process for the preparation of NG-mono-methyl-L-arginine hydrochloride, WO/1997/030972, (1997).
[23] A. Renodon-Corniere, S. Dijols, C. Perollier, D. Lefevre-Groboillot, J.-L. Boucher, R. Attias, M.-A. Sari, D. Stuehr, D. Mansuy, J. Med. Chem. 45 (2002) 944.
[24] L. Fishbein, J.A. Gallaghan, J. Am. Chem. Soc. 76 (1954) 1877.
[25] D.E. Troutner, W.A. Volkert, T.J. Hoffman, R.A. Holmes, Int. J. Appl. Rad. Isot 35 (1984) 467.
[26] J.M. Hevel, M.A. Marletta, Methods Enzymol. 233 (1994) 250.
[27] D.W. Reif, S.A. McCreedy, Arch. Biochem. Biophys. 320 (1995) 170.
[28] J. MacMicking, Q.W. Xie, C. Nathan, Annu. Rev. Immunol. 15 (1997) 323.
[29] N. Lazarova, S. James, J. Babich, Inorg. Chem. Commun. 7 (2004) 1023.
[30] Sadabs, Area-detector Absorption Correction. Brukee AXS Inc., Madison, WI, 2004.
[31] SAINT, Area-Detector Integration Software (Version7.23). Brukee AXS Inc., Madison, WI, 2004.
[32] A. Altomare, M.C. Burla, M. Camalli, G.L. Cascarano, C. Giacovazzo, A. Guagliardi, A.G.G. Moliterni, G. Polidoro, R. Spagna, J. Appl. Crystallogr. 32 (1999) 115.
[33] G.M. Sheldrick, SHELXL-97: Program for the Refinement of Crystal Structure. University of Gottingen, Germany, 1997.
[34] L.J. Farrugia, J. Appl. Cryst. 32 (1999) 837.
[35] L.J. Farrugia, J. Appl. Cryst. 30 (1997) 565.
[36] S. Archer, FASEB J. 7 (1993) 349.
[37] R. Eisenthal, A. Cornish-Bowden, Biochem. J. 139 (1974) 715.
[38] A. Cornish-Bowden, Fundamentals of Enzyme Kinetics, revised ed. Portland Press, 1995.
[39] D.J. Wolff, D.S. Gauld, M.J. Neulander, G. Southan, J. Pharmacol. Exp. Ther. 283 (1997) 265.
[40] R.G. Knowles, S. Moncada, Biochem. J. 298 (1994) 249.
[41] L.C. Green, D.A. Wagner, J. Glogowski, Anal. Biochem. 126 (1982) 131.
[42] T. Mosmann, J. Immun. Methods 65 (1983) 55.